Combined speed control and centralized power supply for hybrid energy-efficient mobile hydraulics

Combined speed control and centralized power supply for hybrid energy-efficient mobile hydraulics

Paola Fresia[a], Massimo Rundo[a,*], Damiano Padovani[b], Gabriele Altare[c]

[a] Politecnico di Torino, 10129, Turin, Italy

[b] Guangdong Technion-Israel Institute of Technology, 515063, Shantou, China

[c] Manitowoc Crane Group Italy S.r.l., 12060, Niella Tanaro, Italy

* Corresponding author: massimo.rundo@polito.it

Abstract

Improving energy efficiency in mobile hydraulics is paramount and feasible via machine electrification, but all actuators' power in standard systems must flow through the electric motors, which is unfeasible for medium-to-high power applications. Therefore, this paper leverages the idea of splitting the transferred power between the hydraulic and electric domains to save energy while downsizing the electric motors. A novel layout of a hybrid excavator is presented, validated using high-fidelity simulations, and compared to the state-of-the-art, load-sensing machine. The results show the expected system's functioning and efficiency benefits (fuel savings close to 28% compared to the original excavator). Almost 60% of the energy is transferred to the actuators hydraulically minimizing the power rating of the electric machines in favor of the system's cost and compactness. Future research will focus on controlling the hybrid system to maximize energy savings and make it easily applicable to different fluid power machines.

Keywords

Energy efficiency, energy recovery, hydraulic excavator, hybrid system, electro-hydraulic system, speed control.

1. Introduction

Environmental and economic motivations require urgent improvements of the energy efficiency in mobile hydraulics. This technology is essential in fields such as earth-moving or construction, where hydraulic excavators are the most popular application. They consume significant amounts of diesel fuel (*e.g.*, over 1 million liters per year in hydraulic mining shovels [1]) releasing carbon dioxide and other pollutants into the atmosphere. Many countries are actively working to limit the consequences for the environment by introducing emission regulations for engines (*e.g.*, Stage V in Europe and EPA Tier 4 Final in the U.S.). Additionally, reducing the fuel consumption of mobile hydraulics has also become an economic issue due to the high price of diesel. State-of-the-art hydraulic systems do not help in this regard despite the multiple system architectures that have been developed over the last decades [2], [3]. The average efficiency of conventional valve-controlled machines is poor due to flow throttling and absence of energy recovery although a limited margin for improvement is still possible [4]. About 12.5% efficiency for the hydraulics alone was calculated for a 5-ton load-sensing (LS) excavator completing digging cycles [5], where about 40% of the losses are given by the control valves and about 20% by the transmission belt and cooling system. For an 18-ton LS machine performing dig-and-dump cycles, the total energy transferred to the actuators was 12.2% of the fuel's energy [6]. Thus, emphasis was focused on including energy recovery in excavators due to the potential savings achievable for the boom and swing drives [7], and to mitigate the abrupt spikes characterizing the power requirements placed on the combustion engine. Some examples are worth mentioning. Multiple hybrid layouts with batteries and/or supercapacitors were introduced [8], [9], even if functional power dissipations in control valves are still commonplace for linear actuators since only the rotary drives are converted to electric actuation. Alternatives that store energy in hydraulic accumulators were also discussed [10], [11], but flow throttling in control valves is still not removed. So, a throttleless actuation with regeneration capabilities was considered for the swing of a hydraulic shovel [12], even if energy-efficiency in the linear actuators of the machine was not addressed. Another valve-controlled approach proposed multiple hydraulic cylinders for the boom drive in combination with a local hydraulic accumulator to store energy locally [13]. The pros and cons of storing energy - using flywheels - were considered as well [14], but this solution alone does not remove the functional power dissipations in control valves.

Alternative system architectures without valves were therefore explored leading to some remarkable solutions. A hybrid active-passive system was studied for the boom drive to hydraulically support an electro-mechanical actuator [15] that ensures good efficiency and controllability but might experience severe limitations in heavy-duty

operations [16]. A nonhybrid displacement-controlled excavator needed only 50% of the LS machine's input energy to complete the same digging cycle [5] and consumed on average 40% less fuel for a truck loading cycle [17]. Fuel savings around 17% were predicted for an updated hybrid version compared to the nonhybrid counterpart [18]. Despite these savings, some drawbacks prevent its dissemination such as the inefficient behavior of pumps at partial displacement, and the costly set-up (at least 4 overcenter pumps controlled by dedicated servovalves). A 21-ton excavator based on digital hydraulics obtained a 36% reduction of the hydraulic input energy compared to the load-sensing counterpart when performing the JCMAS grading cycle [19]. Some control challenges are still not fully resolved (*e.g.*, undesired pressure variations) and many digital valves are needed (112 in this case). Another option combines proportional valves and multi-chamber cylinders on a 30-ton excavator [20]. Measurements indicated a 34–50% better use of the fuel in terms of tons of material moved per liter of diesel, but the flow throttling is not completely removed.

A new and very promising research area regards the electrification of fluid power machines. Speed control is used where a pump, driven by an electric motor, controls the actuator motion efficiently (both throttleless actuation and energy recovery take place). These electro-hydraulic arrangements can easily replace conventional control valves in terms of dynamic response [21] and of energy efficiency [22], [23]. If needed for safety reasons, passive load-holding devices that do not affect efficiency are also available [24]. When it comes to excavators, an example is a 9-ton machine with individual electro-hydraulic drives for the main actuators [25]. The resulting efficiency can increase up to 8.8-14.5% depending on the system design compared to the 5.4% of the LS baseline application. The main drawback is that all the power managed by the actuators must pass through the electric motors: such a solution becomes critical or even infeasible when the power level increases to several kW. A costly arrangement for the electric system (motors, drives, generator, and energy storage device) is also needed and the electric energy must be generated onboard. Thus, hybrid actuators with local energy storage can downsize the rated power of the electric machines [26], but additional components are needed. The same downsizing can be done combining pressure rails supplied by a common pump that are connected to the inlet port of speed-controlled pumps [27]. Power can be transferred to/from the load both hydraulically and electrically, even if the complexity increases dramatically both in terms of system architecture and control effort.

This research paper proposes a hybrid system architecture for mobile machines that avoids functional power losses in control valves to save energy. The article expands the idea of splitting the power transferred to the actuators in a complementary manner between the hydraulic and electric domains. This characteristic enables the electrification of medium-to-high power applications due to the use of low-power electric components, even if the overall power level of the actuators remains unchanged compared to conventional valve control. A novel layout of an excavator is presented where speed-controlled (electro-hydraulic) actuators are supported by a centralized (hydraulic) power supply. As a result, the proposed hybrid system retains the efficiency benefits and control performance of conventional speed control but reduces the amount of electric power used onboard. Therefore the power rating of the electric machines is reduced in favor of the system's cost, compactness, and power density. The proposed hybrid system also has general validity since it is modular, scalable, and applicable to different fluid power machines.

2. Reference hydraulic excavator

2.1 Machine description

The reference vehicle used for this study is a commercial 9-ton excavator with an internal combustion engine capable of providing about 50 kW. The hydraulic circuit feeds five linear actuators shown in Figure 1 and three hydraulic motors for the swing and the two tracks. The hydraulic circuit is based on the load sensing principle with flow sharing.

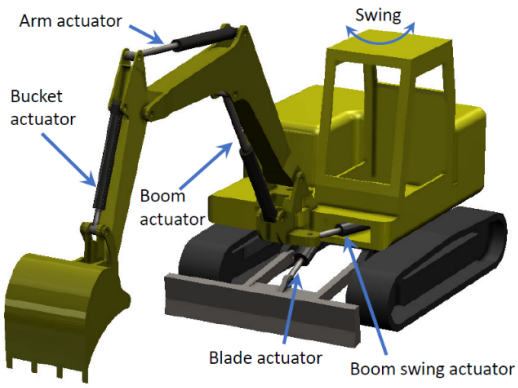

Figure 1. View of the main actuators in the excavator.

The circuit is fed by two pumps driven by the internal combustion engine. A variable displacement axial piston pump (PU1) is equipped with torque limiter and differential pressure limiter controls. A gear pump (PU2) is dedicated to feeding the blade actuator and the swing motor. The pumps are connected to a stack of proportional direction control valves. The simplified scheme is reported in Figure 2, where the modules not of interest in the present study have been omitted.

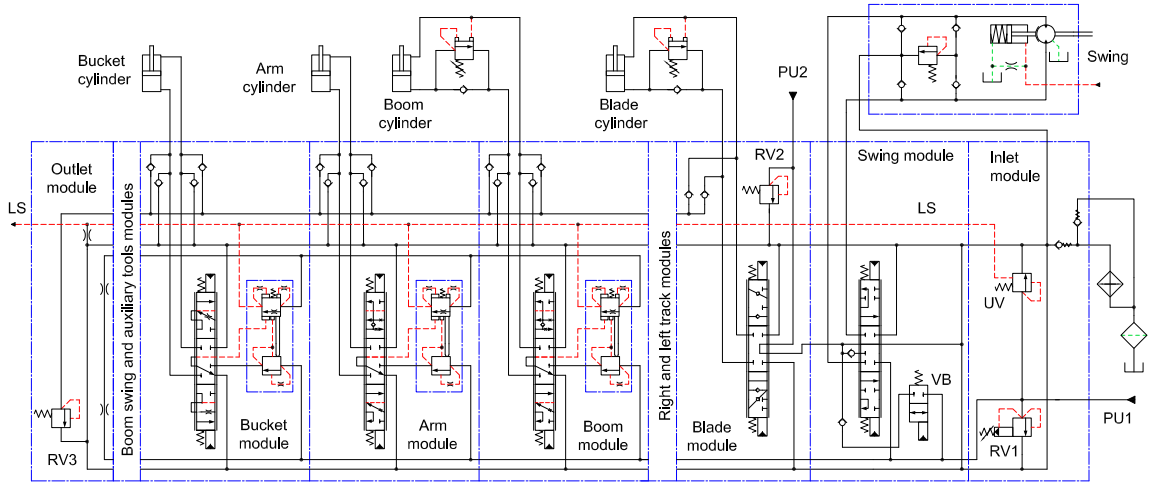

Figure 2. Simplified scheme of the original hydraulic circuit.

The inlet module is connected to the delivery port of the pump PU1 and contains the relief valve RV1 for limiting the maximum pressure, since the pump is not provided with an absolute pressure limiter, and the unloading valve UV for discharging the flow rate in conditions of stand-by. The pump PU2 is connected directly to the blade module, where the relief valve RV2 is present. This pump also feeds the hydraulic swing motor with an integrated holding brake but the blade actuator has priority. In the swing module the boost valve VB is used for increasing the boom velocity when also the hydraulic motor is fed. In fact, when the valve VB is open and the delivery port of the pump PU2 is pressurized, the flow rate delivered to the boom actuator is the sum of the flow rate of the pump PU1 and the residual flow rate of the pump PU2 not used for the swing rotation.

The modules for the boom, arm and bucket are provided with a local compensator that keeps a constant pressure drop across the main spool so that the velocity of the actuators is only function of the valve command supplied by the operator. On the boom and blade actuators an overcenter valve is mounted. Finally, antishock valves are present in the outlet module (RV3) and in the swing motor.

2.2 Simulation model

Simulations have been carried out in the Simcenter Amesim® environment release 2021.1. The model used in the present study, shown in Figure 3 and hereafter referred as the updated model, is an improvement of a previous validated version [28] - hereafter referred as reference model.

In this section only the relevant modifications with respect to the reference model are described in detail, while a summary of the main characteristics is provided for the unchanged parts. Main modifications are relative to the engine and kinematics modelling.

The engine is now modelled with the dedicated library that is more suitable for the connection with the components necessary for the hybrid version presented in the next sections. The model is based on look-up tables deduced from units used for similar applications. Since the same model has been adopted in both architectures under investigation, a representative comparison between the two layouts is feasible. The speed-torque characteristic and the map of fuel consumption as function of the operating conditions are supplied. The speed is not controlled directly because the engine is set to high idle at about 2500 rpm. Therefore, its speed varies according to the maximum torque curve as a load is applied.

The model of the power supply considers both the volumetric and mechanical-hydraulic efficiency of the pumps as function of pressure and speed at constant temperature. For the piston pump the efficiencies at maximum displacement are considered. All displacement controls are simulated in detail considering the real geometry of the pilot valves and of the actuators for tilting the swash plate.

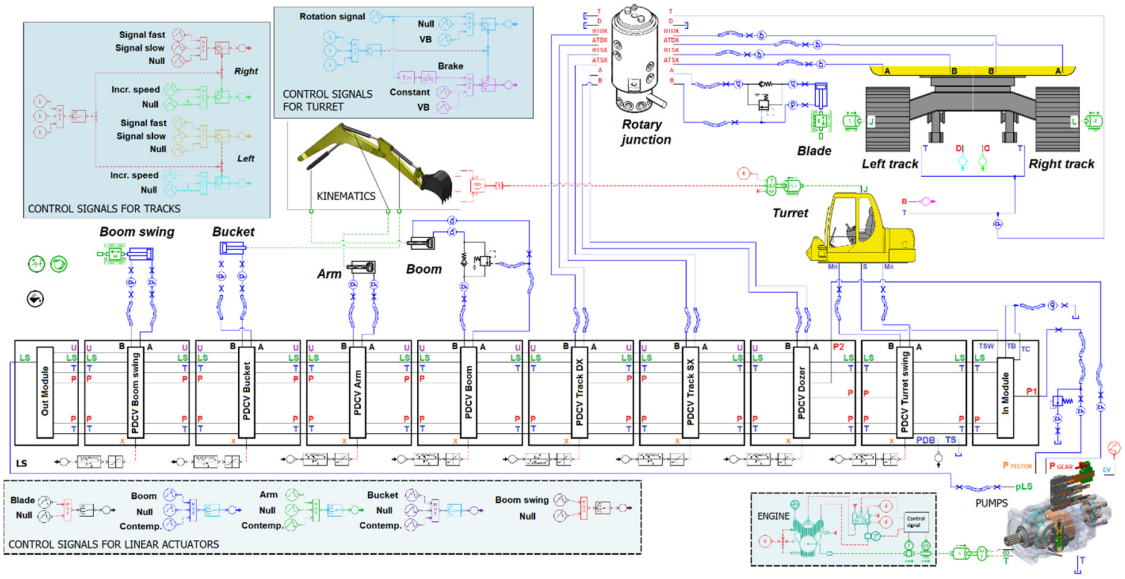

Figure 3. Simcenter Amesim high-fidelity model of the complete hydraulic circuit (nonhybrid excavator).

The directional control valves stack is simulated with the best accuracy by considering all subcomponents. Further details can be found in reference [29]. The linear actuators of boom and arm are simulated by tailor-made supercomponents where the end position cushioning is implemented. The swing model includes the hydraulic motor with integrated holding brake and related valves.

The arm kinematics has been simulated by means of the 2D Mechanical library. In Figure 4 the correspondence between the physical mechanical parts and the model is reported. The bucket model can now compute the digging force on earthy ground and the relative position. This modification allows considering a more realistic load condition with respect to the reference model. The inclination of the soil with respect to the excavator arm can be defined with proper parameters so that both the conditions of unloaded bucket and soil interaction can be simulated. In this way load conditions can be modified since it is possible to obtain different filling factors of the bucket. Additionally, the updated model considers the variation of the cabin inertia as a function of the arm position. Starting from the 3D drawing of the excavator, the inertia of the rotary assembly around the vertical axis was calculated for different values of the arm extension. The x-y coordinates of the hinge C4 are used for computing the current extension of the arm that is used as input of a look-up table for calculating the variation of the inertia. This modelling approach was selected as the best tradeoff between model complexity, result accuracy and computing time.

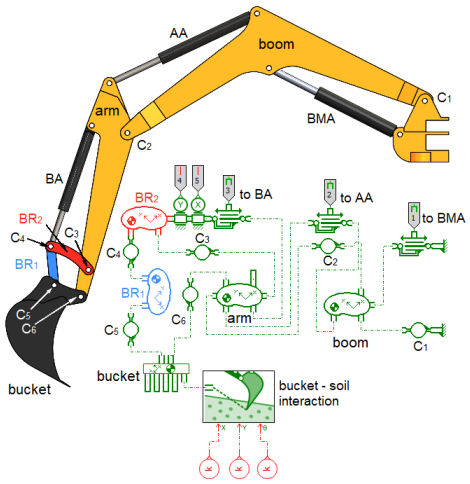

Figure 4. Model of the arm kinematics.

The complete model also includes the circuit for feeding the tracks even if not used in the present study. Finally, the commands to the directional control valves are supplied by proper signal generators for reproducing the desired working cycle.

2.3 Model validation

The reference model of the excavator was validated through experimental tests. The test cycles consisted of supplying the maximum positive and negative command signal to each directional control valve for moving the corresponding actuator. The detailed description of the experimental campaign can be found in reference [28]. In this paper the results of two out of the three actuators involved in the hybridization, namely arm and boom, are reported for showing the reliability of the updated model described in section 2.2. The delivery pressure of the variable displacement pump was measured by a transducer Trafag, with measuring range 0-400 bar and accuracy ± 0.3 % F.S, while the flow rate delivered by the piston pump by a Parker flow meter with measuring range 10-300 L/min and error ±1% of reading. The engine speed was also recorded.

For testing the movement of the arm, the boom was maintained partially lifted and the bucket actuator completely retracted (see the image in Figure 5 for the initial position). The simulated fractional opening of the directional control valve and the arm actuator velocity are plotted in Figure 5a. At time t = 0.5 s the command was supplied until 5.5 s for opening the arm, while between 6.3 and 11.4 s the opposite command was sent for the closing phase. The condition of zero velocity when the command signal is supplied indicates that the actuator has reached the end-stop. The comparison between the simulated and the experimental delivery pressure of the piston pump is shown in Figure 5b. In correspondence of the maximum stroke of the actuator, the system is pressurized at the pressure level imposed by the relief valve RV1. The flow rate generated by the pump is plotted in Figure 5c; it is possible to see a significant flow rate at the maximum pressure level due to the regulation of the relief valve.

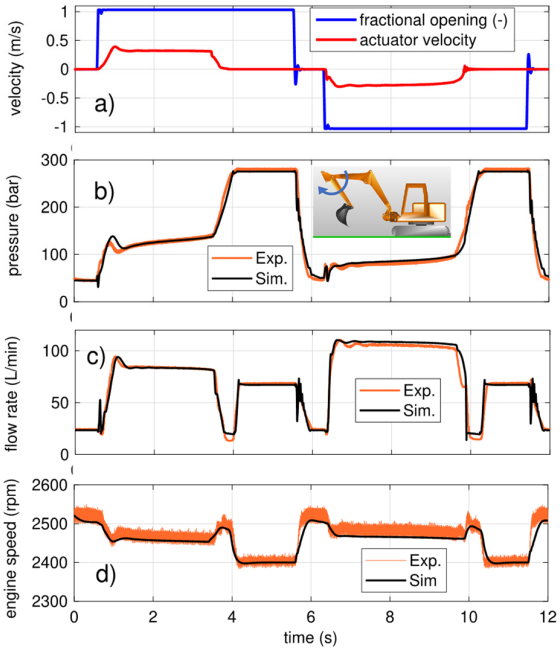

Figure 5. a) Directional valve's fractional opening and actuator velocity, b) delivery pressure, c) flow rate of the piston pump and d) engine speed during the movement of the arm.

For completeness, the delivery pressure of the pump is plotted in Figure 6 during the movement of the boom. The boom test was performed starting with bucket and arm actuators completely retracted and the bucket in contact with the ground. After 2.3 s the command was supplied and maintained until 8.3 s for lifting the boom up to the maximum extension of the actuator. In this operating condition, the load on the actuator is resistive and the behavior is like the case of Figure 5b. The opposite command was sent for lowering the boom between 9.6 and 12.5 seconds. After a pressure peak necessary for accelerating the boom, the pressure level remains lower since the load is overrunning. The last peak at 12.7 s is generated by the contact of the bucket against the ground.

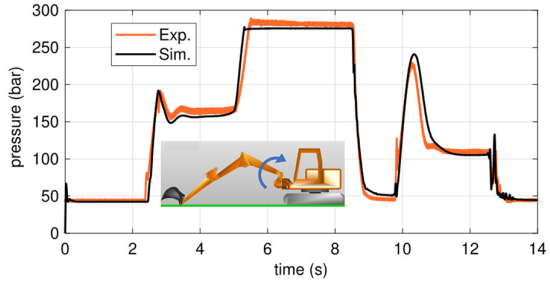

Figure 6. Delivery pressure of the piston pump during the movement of the boom.

Based on the comparison between experimental tests and simulated results, the reliability of the updated model is confirmed. Therefore, with a good degree of confidence, the model can be used for a realistic assessment of the energy consumption of the purely hydraulic architecture and for a comparison with the hybrid solution.

3 Hybrid excavator

3.1 Proposed hydraulic circuit

The goal of the novel system is achieving energy-efficient actuation while ensuring cost-effective implementation. Speed control is proposed because it eliminates flow throttling, enables energy recovery, and favors the electrification of the machine. With conventional speed-controlled architectures, all the power managed by the loads must pass through the electric motors. Such a solution is critical for an excavator because bulky motors and

expensive electronic drives are needed. Then, the electric power must be generated on-board dictating the installation of both a powerful electric generator driven by the combustion engine and a performant energy storage device. For these reasons, the novel system combines electric and hydraulic actuation in a complementary manner. The individual speed-controlled pumps are connected to a centralized hydraulic rail, so a significant amount of power is transferred to the actuators hydraulically. The electric motors still control the motion of the actuators, but they only manage limited amounts of power (*i.e.*, their power ratings are reduced and less electric power is needed on-board).

The layout of the hybrid circuit is shown in Figure 7. The internal combustion engine drives an electric generator G and a fixed displacement pump PU1. The generator is used for charging a supercapacitor-based battery that, in turn, feeds four electric motors. The motor EM4 directly drives the swing, while the units EM1, EM2 and EM3 drive a respective motor-pump MPi.

The pump PU1 along with a gas-charged hydraulic accumulator and the relief valve RV keeps the pressure in the common rail line within a range, so that the hydraulic circuit is fed by an approximatively fixed pressure power supply. If the flow rate generated by the pump exceeds the flow required by the actuators, the excess flow is used for charging the accumulator, regardless of the position of the valve D4, making the pressure in the common rail to increase. When the pressure level has reached the upper value p_M, the pressure switch PS energizes the vent valve of the dual stage pressure relief valve RV and the pump PU1 is depressurized. In this condition, the power absorbed by the pump PU1 is minimized. When at least one actuator is moved, the valve D4 opens and the accumulator can set the pressure in the common rail line. If the pressure falls below the lower limit p_m, PS deactivates the vent stage of the relief valve and the pump can send the flow rate through the valve NR again for directly feeding the actuators. In case of simultaneous movements of all three actuators with high flow requirements, the peak flow is also covered by the accumulator that can supply the amount of volume necessary to complete the strokes. If the engine is shut down the valve D4 is de-energized and by means of the non-return valve, it is possible to avoid the discharge of the accumulator.

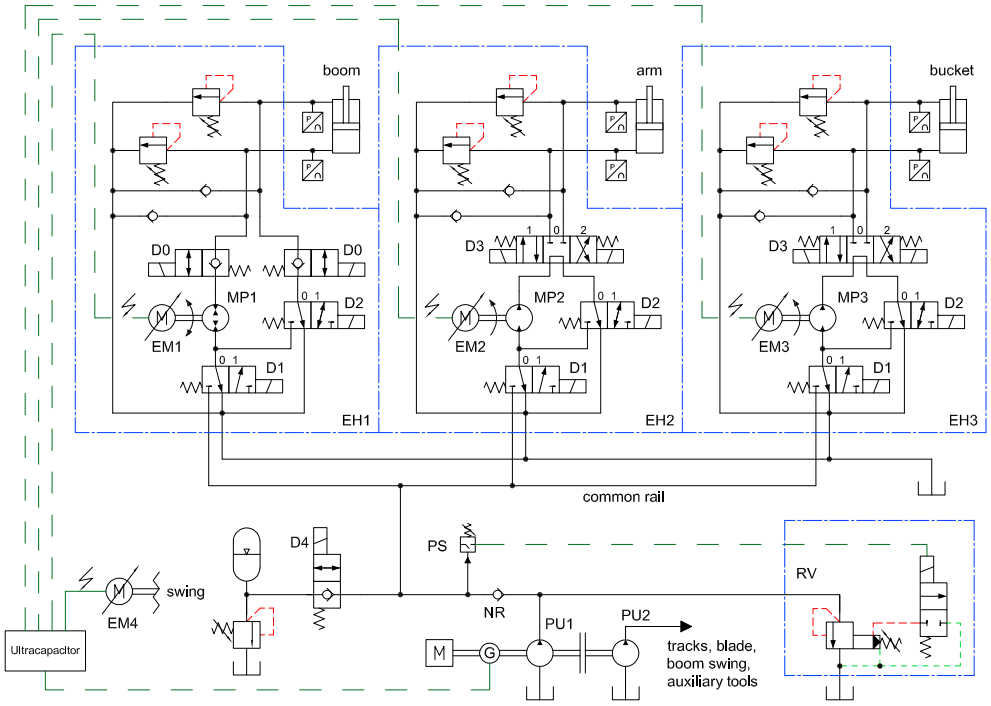

Figure 7. Layout of the proposed hybrid architecture.

The common rail line feeds in parallel the three electro-hydraulic modules EH1, EH2 and EH3 connected respectively to the actuators of boom, arm and bucket. The two valves D0, D1 and D3 are activated simultaneously to the corresponding electric motor by the electronic control unit when the operator gives the command on the joystick.

Hence, there is no difference in the way of controlling the machine and the operator supplies the commands only by means of the joysticks.
The principle is that the machines MPi work in pumping mode, if the pressure imposed by the resistive load on the corresponding actuator is higher than the common rail pressure and the battery supplies power to the electric motor EMi. Vice versa, the hydraulic machine behaves as a motor and the hydraulic power coming from the common rail is converted into mechanical power for driving the electric machine that recharges the battery. The pressure transducers are used to detect if the load is resistive or overrunning to supply a proper signal to the electrovalves D2. The remaining hydraulic linear and rotary actuators (*i.e.*, the track, dozer and boom swing that are not used during standard digging cycles) are fed by the pump PU2 that can be disconnected mechanically when unused for saving energy.

3.2 Working modes

Due to the kinematic of the excavator, different load types in terms of direction and intensity act on the actuators, hence a different layout has been chosen for the boom with respect to the arm and the bucket. In Figure 8 the working modes for the latter actuators are described in four quadrants (QI to QIV).

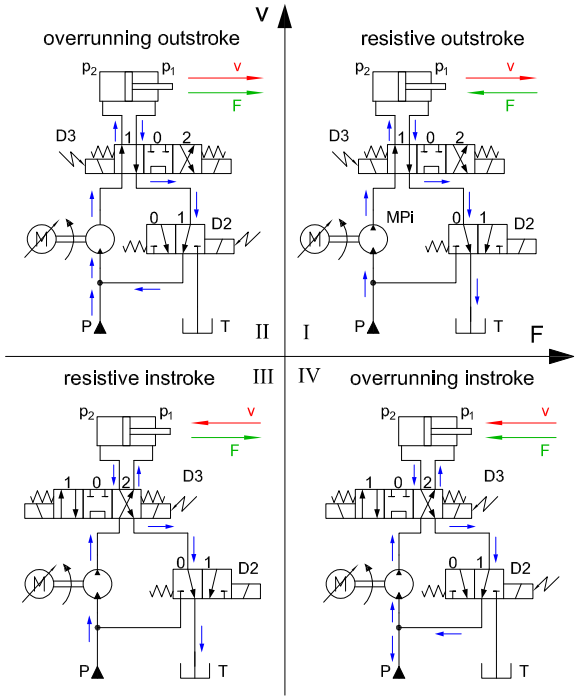

Figure 8. Working modes in four quadrants for the drives of the arm and bucket.

For the extension of the actuator with resistive load (QI) the valve D2 remains at rest and the 4/3 directional control valve D3 is activated in position #1; in this way the path of the oil is from the common rail, through the hydraulic machine and to the bore side chamber of the actuator, while the rod side chamber is connected to the reservoir. As already described, the power flux to or from the electric machine is a function of the load on the actuator. In a similar way, the retraction of the actuator with resistant load (QIII) is obtained by switching the valve D3 in position #2. In both cases the direction of the motion is given by the valve D3, while the actuator velocity is controlled by the electric machine that always rotates in the same direction (this feature is an advantage in those cases where the load changes between resistant and overrunning during the same movement of the piston). If the actuator extends with overrunning load (QII), thanks to the valve D2 it is possible to connect the rod side chamber to the common rail line, so that a backpressure can balance the external force. The pressure in the bore side chamber is a function of the load: the higher the driving force, the lower the pressure. However, the hydraulic machine MPi continues to generate the flow rate as function of the electric motor speed and the controllability of the actuator velocity is guaranteed. The same behavior can be obtained in QIV, with the only difference that the valve D3 is activated in position #2. It is worth noticing that in QII, due to the different areas of the actuator, the pressure in the bore side chamber will be always lower than in the common rail line, therefore the rotary hydraulic machine will behave always as a motor

(*i.e.*, the load energy is recovered hydraulically). On the contrary in QIV, depending on the applied load, the machine can work either as a pump or as a motor. With this architecture, when the load is resistive, the inlet pressure of the actuator can be increased up to the value necessary for generating the maximum force. If it is considered that the pressure at the actuator outlet is ideally the atmospheric one, a significantly high force can be exerted. When the load is overrunning and the actuator is moving outwards, the common rail pressure acts on the smaller surface of the actuator. This is the configuration where the maximum controllable load is the lowest, however the exerted force is sufficiently high for performing all possible operations with the arm and the bucket.
Differently from the arm and the bucket, the boom in a normal digging cycle works only in QI and QIV. Hence it is necessary to optimize the operating condition during the lowering of the boom with overrunning force, although the possibility to work in QII and QIII must be preserved for performing unconventional movements that are sometimes executed by the operators in the field. The specific architecture of the boom circuit is synthesized in Figure 9, where the load-holding valves D0 shown in the general scheme in Figure 7 are omitted for simplicity, since they are always open when a command is given to the electric motor EM1.

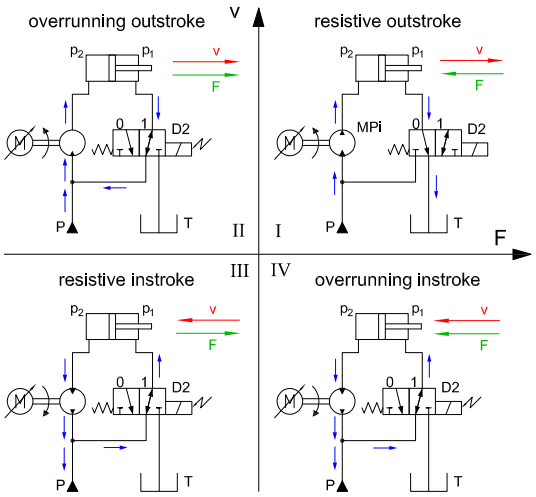

Figure 9. Working modes in four quadrants for the drive of the boom.

The bore side chamber of the actuator is always connected to the rotary hydraulic machine. In QI (boom lifting) the rod side chamber is connected to the reservoir, while the pressure in the bore side chamber can be higher or lower than the common rail pressure depending on the applied load. In QIV, the inversion of the actuator velocity is obtained by inverting the angular velocity of the electric machine and the rod side chamber is pressurized at the common rail pressure thanks to the activation of the valve D2. If the external load is low, the hydraulic machine works as a pump, while high forces can be balanced by the increment of the pressure p_2 up to the maximum allowable value, making possible to recover energy and to always control the actuator velocity.
To make the excavator able to work also in case of unconventional maneuvers, the hydraulic circuit can generate on the boom actuator a significant pressure difference for controlling the speed also in QII and QIII. More specifically, the overrunning force in QII can be balanced by the common rail pressure in the rod side chamber. Since such pressure is also the one at the inlet of the rotary hydraulic machine, due to the area ratio of the actuator, the pressure at the outlet will be lower regardless of the load value letting the rotary hydraulic machine always work as a motor.

3.3 Simulation model

Figure 10 reports the complete simulation model in Simcenter Amesim. The subsystems in common with the reference model are the engine, the arm kinematics and the linear actuators. In the lower part of the circuit, the hydraulic and electric power units are visible. The model of the pump PU1 implements the tabulated volumetric and mechanical-hydraulic efficiencies of a similar unit. The relief valve RV was simulated by considering a flow-pressure characteristic of a typical CETOP 06 component with nominal flow rate 200 L/min. In a similar way, the valves NR and D4 have been sized for managing comparable flow rates, and their flow-pressure characteristics taken from the manufacturer's catalog have been implemented in the respective model. The proper sizing of all valves

minimizes their hydraulic power dissipation. The same geometry of the hoses for the delivery, return and working lines used in the reference model has been reutilized in the circuit of the hybrid excavator. The pressure switch PS is simulated by a trigger, where the two levels p_m and p_M are set. It supplies the activation signal to the vent stage of the relief valve RV.

The electric power unit is simulated by a generator model where the efficiency, as well as the maximum torque and speed, are assumed constant. The energy storage system is simulated by a quasi-static model of a supercapacitor pack that considers the main capacitance, internal resistance and electrical leakage. Transient behavior and the thermal effects are neglected. A logical switch SW is used for enabling the generator based on a lower and upper threshold limit of the supercapacitor state of charge.

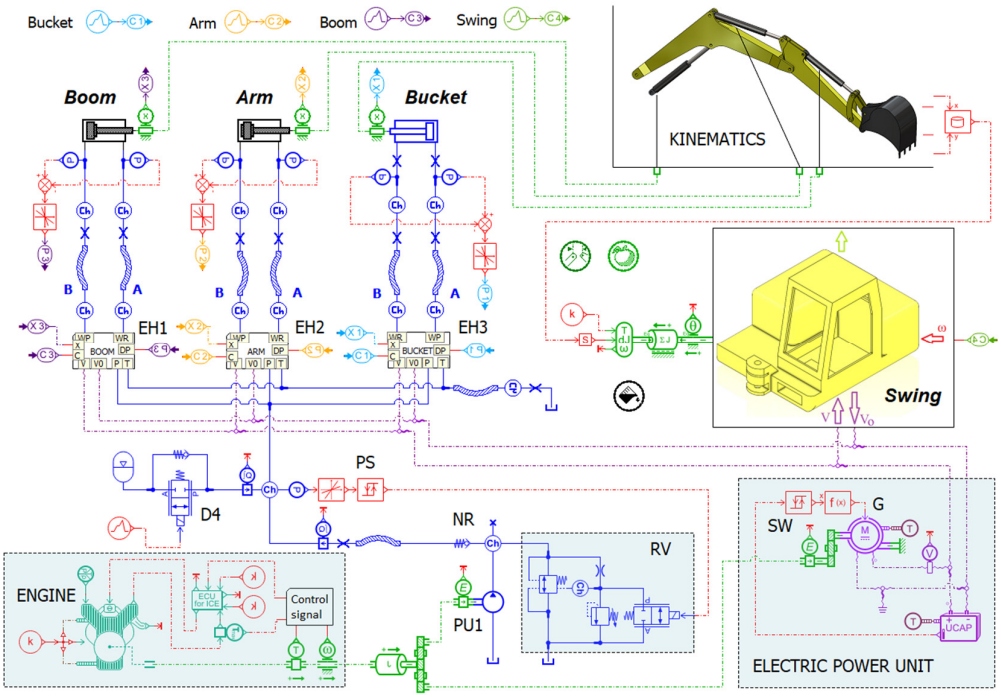

Figure 10. Complete high-fidelity model of the hybrid excavator in Simcenter Amesim.

Table 1 lists the main parameters of the power supply, while Table 2 shows the specifications for the electric power unit. It is worth noting that in the original system the displacements of the axial piston and of the gear pump were respectively 76 and 27 cc/rev.

Table 1. Main parameters of the power supply.

Parameter	Value
Displacement pump PU1	42 cc/rev
Accumulator nominal volume	22.5 L
Accumulator preload pressure	35 bar
Low setting pressure switch PS p_m	70 bar
High setting pressure switch PS p_M	80 bar

Table 2. Main parameters of the electric power unit.

Parameter	Value
Generator power	30 kW
Generator efficiency (constant)	0.9
Supercapacitor nominal voltage	350 V
Supercapacitor electric capacitance	20 F
Supercapacitor specific energy	900 Wh/kg

The electro-hydraulic modules are simulated by supercomponents, one of them is shown in Figure 11. The machine EM is simulated by a functional model of an electric unit where the losses and the torque limits are defined with look-up tables as function of the operating conditions. For this study, the efficiency maps have been supplied by the manufacturer for the selected machines. The motor model receives as input a torque command signal and the actual speed and efficiency are calculated by interpolation of the maps. The unit is reversible and it can work either as a generator or as a motor. For the generator mode, the same maps of the motor have been used. The model of the hydraulic pump-motor MP considers both the volumetric and the mechanical-hydraulic efficiencies; the former is considered by means of equivalent gaps, while the latter with a proper function. The ECU sends the correct commands to the valve D1, D2, and D3 based on the input command supplied by the operator through the joystick and the displacement of the actuators and the pressure drop across them. Such valves are simulated by considering realistic flow-pressure drop characteristics and are controlled with an ON/OFF signal. The electro-hydraulic module EH3 for controlling the bucket is the same, while for the boom the valve D3 is substituted by the valve D0, in accordance with the scheme in Figure 7. It is worth highlighting that all new components, with respect to the model of the reference layout, were simulated by means of functional models, which calculate the output variables as interpolation of real performance data. This approach allows being confident about the accuracy of the energy saving evaluation.

The synthesis of the main parameters is reported in Table 3.

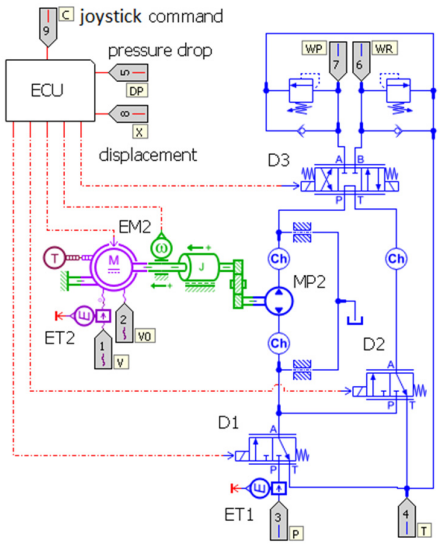

Figure 11. The electro-hydraulic module EH2 of the arm actuator.

Table 3. Main parameters of the electro-hydraulic modules.

Parameter	Value
Displacement MP1	37 cc/rev
Displacement MP2 and MP3	28 cc/rev
Nominal power motor EM1	23 kW
Nominal power motor EM2	8.2 kW
Nominal power motor EM3	8.6 kW
Maximum shaft speed	4000 rpm

4 Comparison between the two layouts

4.1 Test cycle

The two architectures have been evaluated in a trench digging cycle based on the JCMAS standard. Figure 12 shows the displacement of the linear actuators and of the swing as function of time. At the bottom, the solid and hatched bars respectively indicate when a positive and negative command signal is supplied by the joysticks. It must be noted that when the swing rotation is enabled, the speed of the boom increases. This feature in the reference hydraulic system is due to the intervention of the flow boost valve, while in the hybrid version by increasing the speed of the machine MP1. The letters from A to E refer to the excavator positions illustrated in Figure 13. In the hybrid model the input commands have been supplied to electric motors to obtain exactly the same movements of the actuators. In this way the comparison is made rigorously at equal useful mechanical energy.

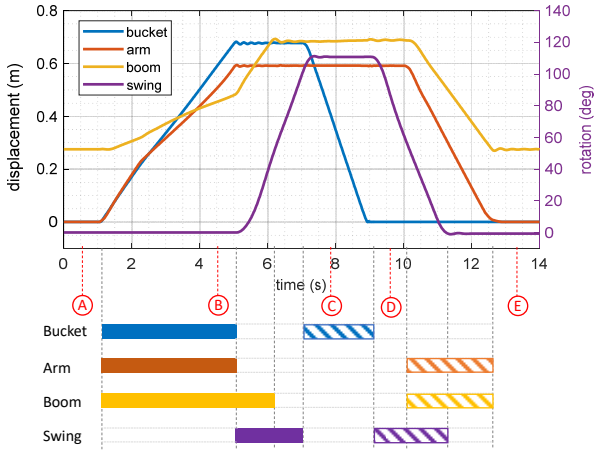

Figure 12. Displacement of the actuators in the digging cycle.

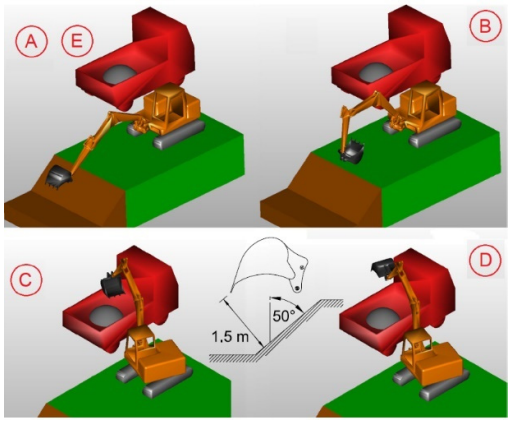

Figure 13. 3D rendering of the relevant excavator positions in the digging cycle.

The soil type named GW - see the Unified Soil Classification System (USCS) - has been selected for the simulation. It is defined as “well graded gravel, sandy gravel, with little or no fines” and has a density of 2141 kg/m^3. Among the classified types of soil, the GW generates the maximum forces of the bucket and therefore the more severe load condition. This configuration has been named “maximum load”. Moreover, the “extreme load” condition has also been defined by setting a very high value of the soil cohesion factor. In this way it is possible to simulate a tool-soil interaction close to facing a fixed obstacle in the ground. Figure 13 shows the slope of the trench and the relative position of the bucket at the beginning of the digging cycle, while Figure 14 depicts the volume of gravel in the bucket as function of time as well as the horizontal and vertical forces on the bucket tip generated by the interaction with the soil.

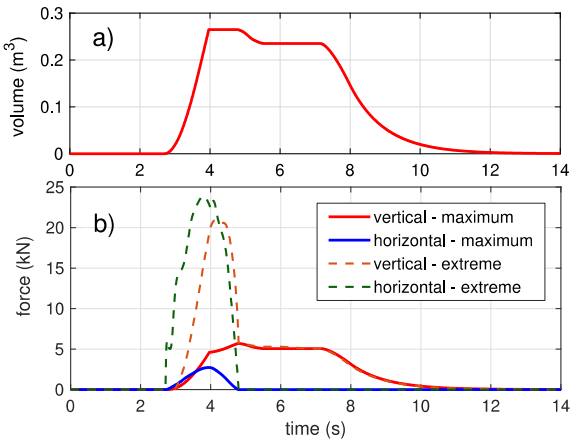

Figure 14. Volume of material in the bucket and forces in the digging cycle.

4.2 Simulated outcomes

The graphs presented in this section show the machine behavior with the proposed architecture. The initial conditions are the accumulator being completely charged (*i.e.*, pressure in common rail equal to 80 bar) and the supercapacitor's state of charge of 85% (simulated scenario #1). For conciseness, only the quantities relative to the arm circuit are shown in detail. The valve D3 is energized simultaneously to the movement of the actuator and defines the direction of motion (Figure 15a). Both ports of the machine MP2 (Figure 15b) are connected to the reservoir during idle. When the valve D1 is actuated, the MP2's inlet port is pressurized at the value of the common rail. During the movement of the actuator, the sign of the pressure difference modifies the behavior of MP2 from motor to pump due to different load conditions, as demonstrated by the inversion of the torque plotted in Figure 15c (being positive for pump behavior).

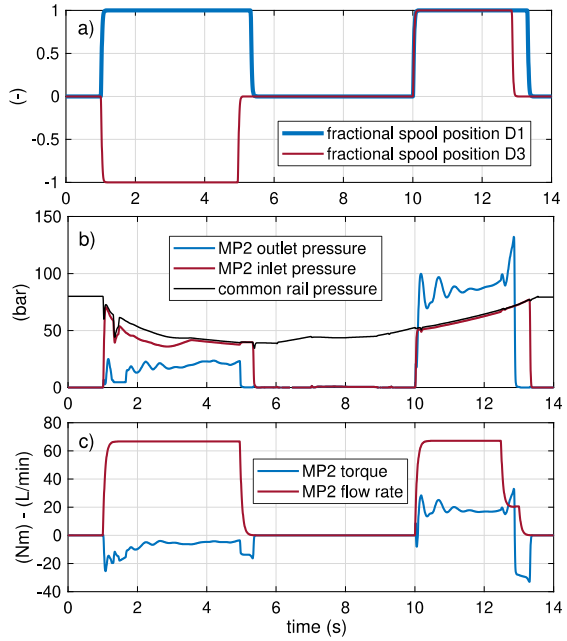

Figure 15. Simulated quantities relative to the arm module EH2 (scenario #1).

The shaft speed of the three hydraulic machines is reported in Figure 16. The units connected to the arm and bucket actuators rotate always in the same direction, while the boom's unit MP1 changes its direction of rotation to invert the movement of the boom cylinder. Moreover, to reproduce the speed increase obtained with the boost valve VB in the original architecture, the MP1 speed is raised accordingly between 5 and 6 s.

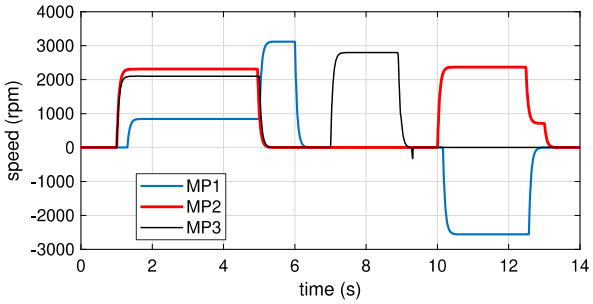

Figure 16. Simulated speed of the hydraulic units MPi (scenario #1).

The quantities relative to the hydraulic power supply are shown in Figure 17. The flow rate for feeding the actuators is initially supplied only by the accumulator since it is fully charged at the beginning of the cycle. As the pressure in the common rail decreases, the vent stage of the relief valve RV is de-energized and an additional flow rate is supplied by the pump. The first part of the cycle - between 1 and 5 s - is the most demanding as the three actuators operate simultaneously at maximum velocity. The pump flow rate is not enough to satisfy the actuators' demands. The accumulator continues to supply flow rate, therefore the pressure in the common rail decreases. At t = 6 s all actuators have reached the end-stop and the entire pump flow rate charges the accumulator. In the second portion of the cycle, a maximum of two actuators are fed simultaneously, hence the pump alone satisfies the flow needs and excess flow is available for recharging the accumulator that is fully charged again before the end of the cycle. The pump is then unloaded.

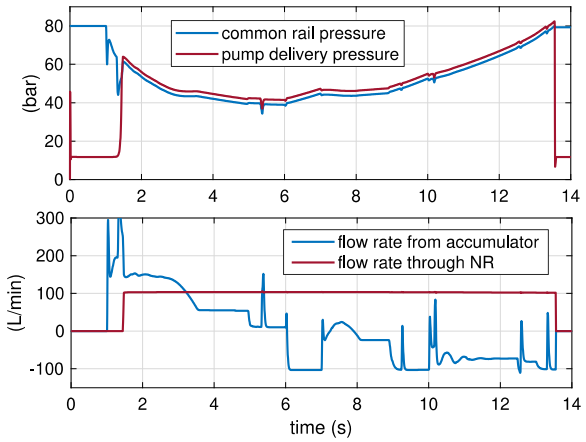

Figure 17. Simulated quantities of the hydraulic power supply (scenario #1).

Focusing the attention on energy exchanges, Figure 18 shows the cumulative energy supplied to the three electro-hydraulic modules. The positive hydraulic term represents the sum of the energy measured by the three transducers ET1 located at the interface between the common rail and the modules (Figure 11), while the positive electric contribution is measured by the three transducers ET2 placed at the electric motors' supply. The negative quantities refer to energies transferred by the modules back to the electric domain and to the common rail. The electric consumption of the additional ON/OFF electrovalves was neglected, being of the order of a few tens of Watt. Considering the values at the end of a single cycle, about 111 kJ are supplied by the common rail and only 66 kJ by the electric power source (63% of the energy is transferred hydraulically and 37% electrically). This situation leads to electric components with reduced rated power as desired (*e.g.,* in the arm drive analyzed above, the peak hydraulic power is about 16 kW, while the maximum electric power only 5 kW).

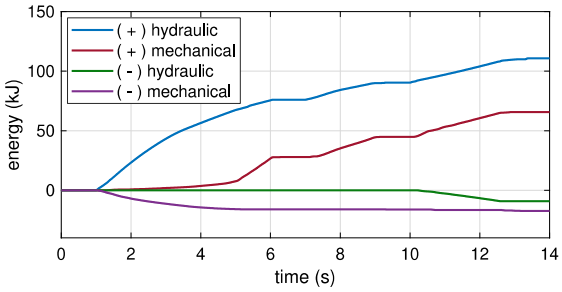

Figure 18. Cumulative energy managed by the electro-hydraulic modules (scenario #1).

To analyze a situation where the electric generator recharges the supercapacitor, a separate simulation of four complete working cycles, 14 s each was performed (scenario #2). It starts with a relatively low state of charge of the supercapacitor equal to 58% (Figure 19a). The first cycle can be completed using the residual stored energy and only the mechanical power necessary to drive the pump is supplied by the engine (Figure 19b). During the second cycle (between 14 and 28 s) the supercapacitor's state of charge reaches the minimum threshold of 50% and the generator recharges it. The generator disconnects when the supercapacitor's state of charge reaches the maximum threshold of 85% during the fourth cycle. As a result, the supercapacitor charges from 50% to 85% in about 26 s and the excavator meet the power demand.

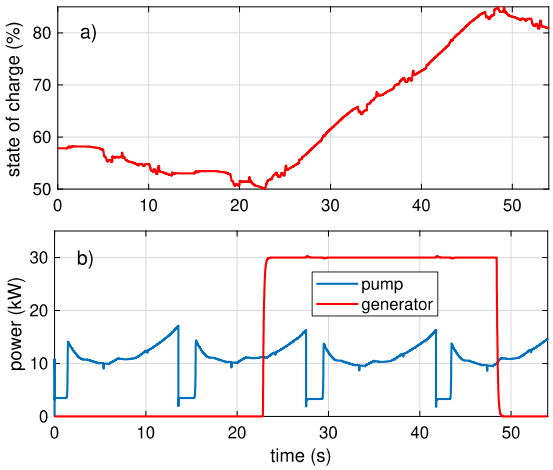

Figure 19. Simulated mechanical and electrical quantities with maximum load (scenario #2).

To compare the advantage of the hybrid architecture with respect to the reference LS system, it is necessary to calculate the average fuel consumption per cycle. In fact, while in the reference circuit there is no energy storage and all cycles are similar, in the hybrid architecture the instantaneous fuel consumption depends also on the operations of the generator. Hence, a new simulation has been performed to obtain a discharge of the supercapacitor from 85% to 50% followed by a charge up to 85%. This simulated scenario #3 repeats several times the same cycle discussed above by modifying both the initial conditions and the load. The average consumption was calculated dividing the total mass of fuel being consumed by the number of digging cycles, in particular 9.45 cycles with the maximum load in the bucket and 11.13 cycles with no load to meet the desired charge/discharge process of the supercapacitor. The condition with no load was obtained by increasing the distance between the tip of the bucket with respect to the trench (Figure 13) to never interact with the soil. The results are synthetized in Table 4 and the fuel savings in both load conditions are always between 26-28%. It is worth mentioning that the actuators of the two systems deliver the same mechanical energy during every cycle, approximately 52 kJ. The reference machine always requires 325 kJ at the engine shaft (*i.e.*, 16% average efficiency). Nevertheless, the hybrid excavator requires less than half energy from the engine, namely 151 kJ, when the generator is not running (frequent condition as stressed in the sequel), or an average of 233 kJ when the engine charges the supercapacitor for about 20% of the total time required to complete these cycles successfully.

Table 4. Average fuel consumption per cycle in both systems (scenario #3).

	Reference	Hybrid	Savings
No load	31.0 g	22.9 g	26.1%
Max load	33.0 g	23.8 g	27.9%

Since the working principle relies on the fact that an amount of energy must be stored either in the accumulator or in the supercapacitor at the beginning of the digging cycle, analyses have been carried out to understand the system behavior in critical charge conditions.

It results that the time for charging the accumulator is negligible (about 5 seconds) when the engine rotates at rated speed and the actuators are not moved, while charging the battery from 5% up to 85% about requires 50 s. If the hydraulic accumulator is fully charged, the digging cycle can be executed at maximum load even with the supercapacitor completely discharged. Obviously in this case, the fuel consumption increases up to about 40 g per cycle since the generator continuously absorbs a significant power until the state of charge of the battery of 85% has been reached. Starting from this unfavorable initial condition, it is interesting to evaluate the number of working cycles after which a fuel saving is obtained with respect to the reference architecture. Figure 20 shows the results of a simulation of multiple cycles with maximum load (simulated scenario #4). At time $t = 0$ s the hybrid system starts with both the accumulator and supercapacitor completely discharged and no actuator is activated until the complete charge (t = 50 s). At this point the digging cycle is started for both architectures and the consumed fuel mass is plotted. Although the hybrid layout is initially in disadvantage, the additional consumption is completely recovered throughout the 14th cycle: hence, from the 15th cycle on, the hybrid architecture allows a fuel saving (it must be noticed that the analyzed situation is the most critical). Recharging the hybrid system before performing actual work does not require any significant modification of the standard procedures. In fact, a minimum wait time between the engine startup and the actual beginning of the digging cycle exists for practical reasons even in the reference system. During this period, fuel is wasted due to the pressure drops in the circuit and other inefficiencies so, the hybrid excavator uses such fuel to recharge the energy storage devices.

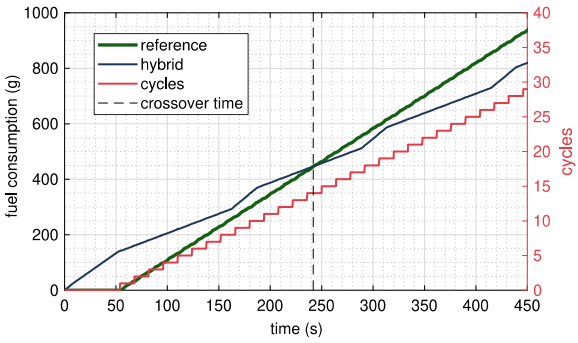

Figure 20. Comparison of cumulative fuel consumptions during working cycles with maximum load (scenario #4), where the hybrid system is, initially, completely discharged.

4.3 Extreme working conditions

While the digging cycle mentioned above represents the standardized sequence of operation that can be used for comparing different machine types, especially from a fuel consumption point of view, it is not representative of all the possible scenarios the excavator can encounter. To make the analysis more robust, additional situations have been considered (*e.g.*, when the bucket hits an obstacle, such as stones or roots) introducing therefore additional resistance to the motion, or when the operator pushes the boom against the ground.

Scenario #5 addresses the first one by simulating again scenario #1 with the load condition labeled as “extreme” in Figure 14b. The high forces due to the interaction between the bucket and the ground generate a significant increment of pressure at the outlet of MP2 in the first stage of the cycle (Figure 21). The electric motor is still able to increase such pressure to a value much higher than the one in the common rail so that the operation can be easily completed.

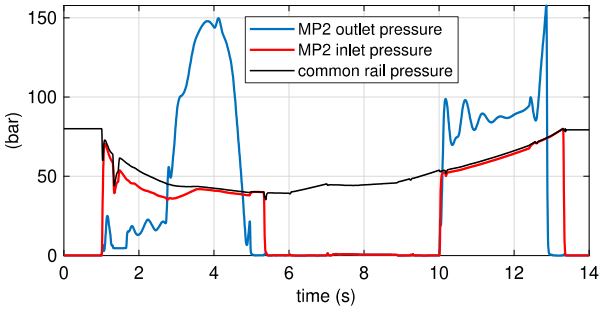

Figure 21. System pressures with extreme load (scenario #5).

The second maneuver that an excavator may encounter is when it pushes the bucket against the ground for compacting the soil or for lifting up the frontal part of the machine to perform, for example an undercarriage rotation by using the swing and one of the tracks (scenario #6). This latter operation is often used by operators for fast path change. This procedure implies the retraction of the boom actuator against a high resistant load (*i.e.*, a fraction of the excavator's weight), as well as the extension with an overrunning load. These load conditions are never reached during normal digging, but the proposed layout can control the actuator velocity in four quadrants. Thanks to the possibility of connecting the rod-side chamber to the common rail and of decreasing the pressure in the bore-side chamber when MP1 works as a pump, a significant force can be exerted in QIII (Figure 9). In a similar way, the possibility to have a backpressure in the boom actuator due to the connection with the common rail allows controlling the overrunning load in QII.

The bucket-soil interaction implemented in the model does not allow for simulating such operating conditions, hence some simplifications have been adopted. The kinematics of the arm has been removed from the model of Figure 10, and a force has been provided as input to the boom actuator by a signal generator. The boom actuator has been actuated alone and the corresponding displacement is shown in Figure 22a.

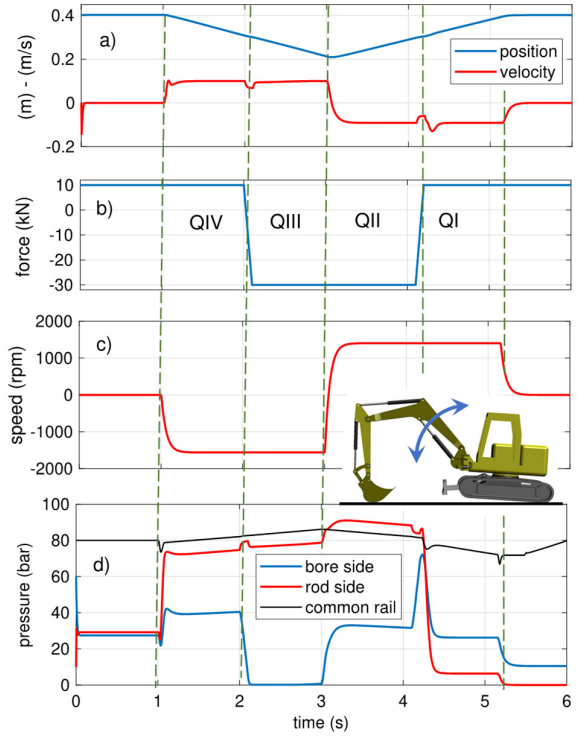

Figure 22. Simulated boom's quantities for scenario #6.

In the time interval between 1 and 3 s the actuator moves inwards with the force input shown in Figure 22b. In this way it is possible to reproduce the working conditions in all four quadrants. In fact, the inversion of the force sign at $t = 2$ s simulates the contact of the bucket against the ground and the subsequent resistant load for lifting the excavator. The load sign's change at $t = 4$ s represents the transition between overrunning and resistant load. As observed in Figure 22c, the speed of the unit MP1 is not influenced by the load inversion - except for negligible transients, the actuator velocity remains basically unchanged despite the significant variation of the load. Finally, in Figure 22d the pressures in the chambers of the boom actuator and in the common rail are shown.

The latter results ensure therefore the excavator can perform even in corner cases and prove the general validity of the proposed hybrid system.

Conclusions

This research paper addresses the crucial issue of improving the machines' energy efficiency in mobile hydraulics. It presents and validates a novel layout of a hybrid, electro-hydraulic excavator capable of throttleless actuation and energy recovery. The new system has the peculiarity of splitting the power being transferred to/from the actuators between the hydraulic and electric domains; this aspect is key to enable the electrification of medium-to-high power applications. High-fidelity simulations support this study that delivers the following main results:

1) The hybrid excavator meets the performance of the original valve-controlled machine in terms of actuator motion and delivered force for a variety of working conditions, both standard and extreme.
2) The hybrid excavator transfers to the actuators about 63% of the energy hydraulically and only 37% electrically during representative digging cycles (scenario #1). The benefits of the electrification are maintained, but the power rating of the electric machines is minimized (*e.g.,* the peak hydraulic power is about 16 kW in the arm drive, while its maximum electric power is only 5 kW).
3) The hybrid excavator can complete working cycles characterized by demanding load conditions even with a partial charge of the energy storage device (scenario #2). In this situation, it can even increase the supercapacitor charge from 50% to 85% in about 26 s.
4) The hybrid excavator ensures, on average, fuel savings between 26-28% compared to the load-sensing version (scenario #3). These numbers refer to comprehensive operating cycles with different load conditions and varying charging states of the energy storage devices.
5) The hybrid excavator can recharge the supercapacitor from 5% to 85% in 50 s and the hydraulic accumulator in a few seconds without requiring any significant modification of the standard operating procedures. In this case, fuel savings take place after 14 digging cycles (scenario #4).
6) The hybrid excavator can also meet extreme working conditions such as severe bucket/soil interactions (scenario #5) or operating the boom actuator in four quadrants (scenario #6).

In short, the proposed hybrid system behaves as expected in diverse operations and leads to important energy savings during typical digging. Its full capability of replacing state-of-the-art excavators is reinforced by the reduced rated power of the electric machines (*i.e.*, cost effectiveness and minimum onboard generation of electricity) that counteracts the need of installing additional components. The implications of such a result are powerful: they show that the research community can come up with valid ideas that give to fluid power manufacturers the opportunity to take action in limiting the emissions of carbon dioxide and other pollutants into the atmosphere. Future research will focus on advanced control of the hybrid system to maximize the energy savings, downsize the combustion engine, and empower the system's general validity. In fact, this architecture based on a modular and scalable design is attractive for multiple fluid power applications such as wheel-loaders, cranes, and telehandlers.

Acknowledgements

The authors acknowledge the support of Bonfiglioli SpA for providing the efficiency maps of the electric motors used in the simulations. The authors thank Sara Altare for her help with English editing.

References

[1] Z. Quan, L. Ge, et al., "A Survey of Powertrain Technologies for Energy-Efficient Heavy-Duty Machinery," Proceedings of the IEEE, **109**(3): 279-308, 2021, doi: 10.1109/JPROC.2021.3051555.

[2] D. Padovani, M. Rundo and G. Altare, "The working hydraulics of valve-controlled mobile machines: Classification and review," J. Dyn. Syst. Meas. Control Trans. ASME **142**(7): 1-15, 2020, doi: 10.1115/1.4046334.

[3] A. Bedotti, M. Pastori and P. Casoli, "Modelling and energy comparison of system layouts for a hydraulic excavator," Energy Procedia **148**:26-33, 2018, doi: 10.1016/j.egypro.2018.08.015.

[4] A. Gaiola, B. Zardin et al. "The Hydraulic Power Generation and Transmission on Agricultural Tractors: Feasible architectures to reduce dissipation and fuel consumption-Part I," E3S Web of Conferences, **197**, 2020, doi: 10.1051/e3sconf/202019707009.

[5] J. D. Zimmerman and M. Ivantysynova, "Reduction of Engine and Cooling Power by Displacement Control," Proceedings of the 6th FPNI-PhD Symposium, West Lafayette, USA, 2010.

[6] M. Vukovic, R. Leifeld and H. Murrenhoff, "Reducing fuel consumption in hydraulic excavators-a comprehensive analysis," Energies **10**(5), 2017, doi: 10.3390/en10050687.

[7] A. Hießl and R. Scheidl, "Energy consumption and efficiency measurements of different excavators - Does hybridization pay?," ASME/BATH Symposium on Fluid Power and Motion Control, Chicago, USA, 2015, doi: 10.1115/FPMC2015-9568.

[8] T. Lin, Q. Wang, B. Hu and W. Gong, "Research on the energy regeneration systems for hybrid hydraulic excavators," Autom. Constr. **19**(8):1016-1026, 2010, doi: 10.1016/j.autcon.2010.08.002.

[9] H. Wang, Q. Wang and B. Hu, "A review of developments in energy storage systems for hybrid excavators," Autom. Constr. **80**:1-10, 2017, doi: 10.1016/j.autcon.2017.03.010.

[10] S. Li, J. Wei, et al., "Design and control of hydraulic hybrid system for excavators," ASME/BATH Symposium on Fluid Power and Motion Control, Chicago, USA, 2015, doi: 10.1115/FPMC2015-9564.

[11] P. Casoli, A. Gambarotta, N. Pompini and L. Riccò, "Hybridization methodology based on DP algorithm for hydraulic mobile machinery - Application to a middle size excavator," Autom. Constr. **61**: 42-57, 2016, doi: 10.1016/j.autcon.2015.09.012.

[12] J. Huang, Z. Dong, et al., "Development of a dual displacement controlled circuit for hydraulic shovel swing motion," Autom. Constr. **57**:166-174, 2015, doi: 10.1016/j.autcon.2015.06.006.

[13] G. Jun, Z. Daqing, et al., "Potential energy recovery method based on alternate recovery and utilization of multiple hydraulic cylinders," Autom. Constr **112**, 103105, 2020, doi: 10.1016/j.autcon.2020.103105.

[14] J. Li and J. Zhao, "Energy recovery for hybrid hydraulic excavators: flywheel-based solutions," Autom. Constr. **125**, 103648, 2021, doi: 10.1016/j.autcon.2021.103648.

[15] Z. Li, C. Wang, et al., "Study on energy efficiency characteristics of the heavy-duty manipulator driven by electro-hydraulic hybrid active-passive system," Autom. Constr. **125**, 103646, 2021, doi: 10.1016/j.autcon.2021.103646.

[16] D. Hagen, D. Padovani, M. Choux, "Guidelines to Select between Self-Contained Electro-Hydraulic and Electro-Mechanical Cylinders," Proceedings of the 15th IEEE Conference on Industrial Electronics and Applications, Virtual, 2020, doi: 10.1109/ICIEA48937.2020.9248373.

[17] J. Zimmerman, E. Busquets and M. Ivantysynova, "40% Fuel Savings by Displacement Control Leads to Lower Working Temperatures - A Simulation Study and Measurements," Proceedings of the 52nd National Conference on Fluid Power, Las Vegas, USA, 2011.

[18] R. Hippalgaonkar, M. Ivantysynova and J. Zimmerman, "Fuel savings of a mini-excavator through a hydraulic hybrid displacement controlled system," Proceedings of the 8th International Fluid Power Conference, Dresden, 2012.

[19] M. Ketonen and M. Linjama, "Digital hydraulic IMV system in an excavator - first results," Proceedings of the 16th Scandinavian International Conference on Fluid Power, Tampere, Finland 2019. Available at https://trepo.tuni.fi/handle/10024/117427.

[20] K. Heybroek and M. Sahlman, "A hydraulic hybrid excavator based on multi-chamber cylinders and secondary control–design and experimental validation," Int. J. Fluid Power **19**(2): 91-105, 2018, doi: 10.1080/14399776.2018.1447065.

[21] D. Hagen, D. Padovani and M. Choux, "A comparison study of a novel self-contained electro-hydraulic cylinder versus a conventional valve-controlled actuator-part 1: Motion control," Actuators **8**(4). 2019, doi: 10.3390/ACT8040079.

[22] D. Hagen, D. Padovani and M. Choux, "A comparison study of a novel self-contained electro-hydraulic cylinder versus a conventional valve-controlled actuator-part 2: Energy efficiency," Actuators **8**(4), 2019, doi: 10.3390/ACT8040078.

[23] S. Qu, D. Fassbender, A. Vacca and E. Busquets, "A high-efficient solution for electro-hydraulic actuators with energy regeneration capability," Energy, **216**: 119291, 2021, doi: 10.1016/j.energy.2020.119291.

[24] D. Padovani, S. Ketelsen, D. Hagen and L. Schmidt, "A self-contained electro-hydraulic cylinder with passive load-holding capability," Energies **12**(2), 2019, doi: 10.3390/en12020292.

[25] P. Casoli, F. Scolari, T. Minav and M. Rundo, "Comparative energy analysis of a load sensing system and a zonal hydraulics for a 9-tonne excavator," Actuators **9**(2), 2020, doi: 10.3390/ACT9020039.

595 [26] D. Padovani, S. Ketelsen and L. Schmidt, “Downsizing the electric motors of energy-efficient self-contained electro-
596 hydraulic systems by using hybrid technologies,” BATH/ASME Symposium on Fluid Power and Motion Control, Bath, UK,
597 2020, doi: 10.1115/FPMC2020-2717.
598 [27] P. Y. Li, J. Siefert and D. Bigelow, “A hybrid hydraulic-electric architecture (HHEA) for high power off-road mobile
599 machines,” ASME/BATH Symposium on Fluid Power and Motion Control, Longboat Key, USA 2019, doi:
600 10.1115/FPMC2019-1628.
601 [28] G. Altare, D. Padovani and N. Nervegna, “A Commercial Excavator: Analysis, Modelling and Simulation of the Hydraulic
602 Circuit,” SAE Technical Paper 2012-01-2040, 2012. doi: 10.4271/2012-01-2040.
603 [29] G. Altare, D. Padovani and N. Nervegna, “A Close-up View of a Load Sensing ‘Hybrid’ Proportional Directional Control
604 Valve,” Transactions of the Japan Fluid Power Systems Society **44**(3): 64-73, 2013. DOI: 10.5739/jfps.44.64.